Ukrainian Journal of Physical Optics
ISSUE 2
2026

Vibrational Cooling of RbCs Molecules

Omama Al Kharusi [1,2,T], Ridha Horchani [1,T*], Uduakobong S. Okorie [3],
Akpan N. Ikot [4]

[1] Department of Physics, College of Science, Sultan Qaboos University, P.O. Box 36,
Al-Khod, P. C. 123, Muscat, Sultanate of Oman
[2] Department of Applied Mathematics and Science, National University of Science and Technology,
Al Hail, Al Seeb, 111, Muscat, Sultanate of Oman
[3] Department of Physics, University of South Africa, Florida, 1710, Johannesburg, South Africa
[4] Theoretical Physics Group, Department of Physics, University of Port Harcourt,
Rivers State, Nigeria.
* Corresponding author: horchani@squ.edu.om
[T] These authors contributed equally to this work

Received: 27.08.2025

Abstract. We theoretically investigate the vibrational cooling of RbCs molecules formed via the photoassociation of Rb and Cs atoms. A sample of cold molecules, initially distributed across multiple vibrational levels, can be transferred into a specific vibrational level of the singlet ground electronic state, $X^1\Sigma^+$. This is achieved by repeated optical pumping with a laser light spectrum broad enough to excite all populated vibrational levels except the target one. The results show that this cooling method achieves an efficiency of nearly 90 %.

Keywords: optical pumping, vibrational cooling, molecules
UDC: 621.373.826
DOI: 10.3116/16091833/Ukr.J.Phys.Opt.2026.02023

1. Introduction

The ability to precisely control both the internal and external degrees of freedom of molecules is highly promising and offers the potential for significant breakthroughs across different areas of physics [1, 2] and modern physical chemistry [3, 4]. From an experimental perspective, it is well established that molecules are more challenging to manipulate than atoms because of their internal complexity. This challenge has led to the theoretical development of innovative control methods, including those aimed at manipulating the internal degrees of freedom of (cold and ultracold) molecules [5–7]. Long-range interactions and quantum effects dominate dense molecular gas systems, making them an ideal platform for simulating solid-state behavior with exceptional control and accuracy, enabling the study of phenomena such as superconductivity and the discovery of new phases of matter [8–11].

Experimentally, producing a dense, cold molecular sample remains highly challenging for most species beyond a limited set. Existing methods in the literature generally fall into two categories. The first involves forming molecules from pairs of ultracold trapped atoms, achieved either through magnetoassociation (MA) using a magnetic Feshbach resonance (MFR) followed by optical transfer to the ground state [12–16], or via photoassociation with subsequent radiative emission [17–20]. While these techniques can generate cold molecular samples of around 10^5 molecules at temperatures between 0.2–50 μK, they are restricted to species that can be laser-cooled. The second category involves direct applications for the production of cold molecules, such as collisions with a cold buffer gas [21] or the use of external electric [22–24], magnetic [25–27], or optical fields [28]. These methods typically produce dilute molecular samples at millikelvin temperatures.

Cold polar molecules are a cornerstone for emerging applications in quantum simulation [10], quantum computation, quantum chemistry, and precision measurement [29–36]. This potential has attracted researchers from various scientific disciplines, such as atomic, optical, and condensed matter physics, physical chemistry, and quantum science, to work together to produce high-density samples of these molecules in their absolute rovibronic ground state. To this end, significant progress has been made. The most successful experiments often employ a pulsed technique that involves magnetoassociation of Feshbach molecules, followed by coherent transfer to the ground state via stimulated Raman adiabatic passage (STIRAP) [13, 37, 38]. An alternative route is direct photoassociation, in which spontaneous emission populates deeply bound states, a method demonstrated for various molecules, including KRb [39], LiCs [40], RbCs [41–44], and NaCs [45], and explored theoretically in Ref. [46].

Despite these successes, a significant challenge persists. The formed molecules are typically produced in a distribution of vibrational levels within the electronic ground state, rather than exclusively in the lowest vibrational level ($v''=0$). The population of higher vibrational states limits the lifetime of the molecular sample due to inelastic collisions and spontaneous decay, and prevents the attainment of a pure, long-lived quantum gas in the absolute rovibronic ground state. This state is a prerequisite for most high-precision experiments, including those probing fundamental physics, quantum simulation, and quantum computation. Therefore, developing an efficient scheme for vibrational cooling such as a transfer of population from these higher-lying vibrational states ($v''>0$) down to the absolute ground state ($v''=0$) remains a critical challenge. While strategies such as optical pumping have been considered, a detailed theoretical proposal for a robust, multi-cycle optical cooling scheme specifically tailored to RbCs has been lacking.

In this work, we address this gap by proposing and theoretically analyzing a path toward efficient vibrational cooling of RbCs molecules. Our scheme is based on optical transitions between the ground $X^1\Sigma^+$ state and the excited $B^1\Pi$ state, driven by a spectrally shaped broadband laser centered at 732 nm. This specific transition is particularly advantageous for two reasons. First, the relatively short lifetime of the excited state (~12 ns) allows for the high photon-scattering rates required for efficient cooling. Second, the Franck-Condon factors (FCFs) between these states are highly favorable for closing the optical cycle. Building on foundational laser-cooling work in other molecules [47–60], our proposed scheme offers a practical route to producing pure, ultracold RbCs samples for next-generation precision spectroscopy and quantum simulation experiments.

2. Simulation

The core idea behind the optical pumping method, as implemented in [41, 43–55], involves using a broadband laser tuned to address transitions between vibrational levels denoted v_X and v_B, which correspond to levels in the singlet ground electronic state $X^1\Sigma^+$ (hereafter referred to as X) and the electronically excited state $B^1\Pi$ (hereafter referred to as B), respectively, of the RbCs molecule (see Fig. 1a). Fig. 1b illustrates the FCFs, which represent the squared normalized overlaps between the vibrational wavefunctions for transitions from vibrational levels v_X of the ground state X to levels v_B of the excited state B. The FCF distribution is non-diagonal; that is, the transition $v_X = 0 \leftrightarrow v_B = 0$ is not the most probable. Instead, the highest FCF is observed for the $v_X = 0 \leftrightarrow v_B = 2$ transition, with a value of 0.26597 [52].

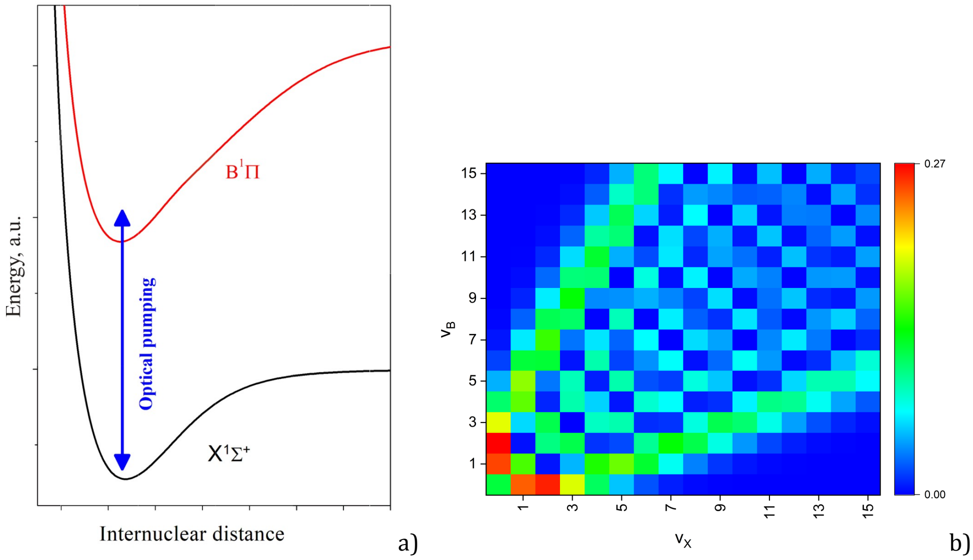

Fig. 1. (a) Schematic diagram for RbCs $X^1\Sigma^+$ and $B^1\Pi$ potential energy curves used in the proposed cooling scheme. (b) Franck-Condon Factors (FCFs) for transitions between the $X^1\Sigma^+(v_X)$ vibrational levels and the $B^1\Pi(v_B)$ vibrational levels.

The goal is to begin with an initial distribution of molecules across different vibrational levels, v_X, and transfer them to a single selected target level. This is achieved through cycles of absorption and spontaneous emission, which, via optical pumping, redistribute the vibrational population in the ground electronic state. The process follows the general scheme:

$$\mathrm{RbCs}(v_X) + h\nu_{las} \rightarrow \mathrm{RbCs}(v_B) \rightarrow \mathrm{RbCs}(v'_X) + h\nu_{em}, \tag{1}$$

where $h\nu_{las}$ and $h\nu_{em}$ are the energies of the laser and of the spontaneously emitted photons, respectively. v'_X is the vibrational level after spontaneous emission. The broadband laser spectrum enables pumping from multiple vibrational levels v_X. Selective removal of excitation frequencies for a specific v_X level renders it a dark state by preventing further depopulation. Over time, repeated absorption and spontaneous emission cycles, as described by Eq. 1, result in the accumulation of molecules in the target vibrational level, v'_X.

To model the process, the optical pumping cycle is divided into two steps: excitation from the ground state X to the excited state B (absorption), followed by spontaneous emission from B back to X. The short pulse duration allows us to disregard spontaneous emission during absorption, as its impact on the final population distribution is negligible. Similarly, stimulated emission is omitted due to the low laser intensity. Based on the known potential curves and rotational constants of the molecular system, we compute the ro-vibrational energy levels and FCFs for the transitions. The average laser intensity is sufficiently weak to operate in a perturbative regime, meaning the excitation probability depends linearly on the laser spectral density at the transition frequencies, the FCF, and the Hönl-London factor (HLF). Given the excited-state lifetime of 15 ns, fewer than one photon is absorbed per pulse, ensuring complete population decay before the next pulse arrives (after 12.5 ns). Additional processes, such as broadband laser-induced three-photon direct ionization and predissociation, are also included in the simulation.

In the perturbative regime (i.e., under low laser intensity), the distribution of molecules across the various vibrational levels during the absorption step is described by:

$$\begin{aligned} \mathrm{P}_{v_X}^{(n+1)} &= \mathrm{P}_{v_X}^{(n)} - \sum_{v_B} A_{v_B v_X} \mathrm{P}_{v_X}^{(n)}, \\ \mathrm{P}_{v_B}^{(n+1)} &= \sum_{v_X} \mathrm{A}_{v_B v_X} \mathrm{P}_{v_X}^{(n)}, \end{aligned} \tag{2}$$

and in emission by

$$\mathrm{P}_{v_X}^{(n+2)} = \mathrm{P}_{v_X}^{(n+1)} + \sum_{v_B} E_{v_X v_B} \mathrm{P}_{v_B}^{(n+1)}. \tag{3}$$

where $P_{v_X}^{(n)}$ and $P_{v_B}^{(n)}$ represent the populations of vibrational levels v_X and v_B at the n^{th} stage of the process.

$A_{v_X v_B}$ denotes the fraction of the molecular population transferred from a vibrational level v_{X} in the ground state to a level v_{B} in the excited state, within the range accessible by the laser bandwidth. Similarly, $E_{v_X v_B}$ represents the fraction of the population that decays via spontaneous emission from an excited vibrational level v_B to a level v_X. These rates are proportional to the corresponding FCFs, $q_{v_X v_B}$, the transition dipole moments, $(D_{v_X v_B})^2$, and transition frequency of the vibrational transition, $\omega_{v_X v_B}$: $A_{v_X v_B} \propto q_{v_X v_B}(D_{v_X v_B})^2 I_{las,v_X v_B}$ and $E_{v_X v_B} \propto q_{v_X v_B}(D_{v_X v_B})^2 \omega_{v_X v_B}^3$, where $I_{las,v_X v_B}$ is the laser intensity.

As a consequence, after N steps of absorption-spontaneous emission cycles, we obtain

$$P(2N) = M^N P(0), \tag{4}$$

with $M_{ij} = (1+EA)_{ij} - \sum_k A_{ki}\delta_{ij} = \delta_{ij} + \sum_k (E_{ik}A_{kj} - A_{ki}\delta_{ij})$ where, E and A represent the population fractions decayed via spontaneous emission and gained by absorption, respectively. The indices *i*, *j*, and *k* denote the vibrational levels at each stage of the process (*i* is the initial vibrational level in the ground *X* state, *j* is the vibrational level in the excited *B* state after absorption, and *k* is the final vibrational level in the *X* state after spontaneous emission. For example, a very simple optimization procedure to pump toward a single level v_0 can only consider that the laser intensity ($I_{las,v_X v_B}$) can be either ON or OFF. We can then write $\mathrm{A}_{ij} = \mathrm{A}_{ij}\Delta_{ij}$, where $\Delta_{ij} = 0$ when the laser component is turned OFF and 1 when it is turned ON.

The criterion for convergence is that the population in stage number 2, $\mathbf{P}^{(2)}$, has to get closer to $\mathbf{P}_0$, a target distribution defined by $(P_0)_i = \delta_{iv_0}$, where v_0 is the target vibrational level. This means that we have to minimize the norm

$$\begin{aligned} L_1 &= \| P(2) - P_0 \|_1 = 1 - P^{(2)}_{v_0} + \sum_{v_X \neq v_0} P^{(2)}_{v_X} \\ &= 1 - P^{(2)}_{v_0} + \sum_{v_X \neq v_0} P^{(0)}_{v_X} \\ &+ \sum_{v_B v'_X} \Delta_{v_B v'_X} A_{v_B v'_X} P^{(0)}_{v'_X} \sum_{v_X \neq v_0} (E_{v_X v_B} - \delta_{v_X v'_X}). \end{aligned} \tag{5}$$

We note that if $v'_X = v_0$ and $\sum_{v_X \neq v_0} \left(\mathrm{E}_{v_X v_B} - \delta_{v_X v'_X} \right) > 0$, we have to set $\Delta_{v_B v_0} = 0$. This ensures that the target level v_0 is a dark state and cannot interact with the laser. On the other hand, if $v'_X \neq v_0$ and $\sum_{v_X \neq v_0} \left(E_{v_X v_B} - \delta_{v_X v'_X} \right) < 0$, minimizing the norm, L_1, means $\Delta_{v_B v_{X'}} = 1$. In this case, the laser is switched ON to excite all molecules in vibrational levels $v'_X \neq v_0$.

The laser must be sufficiently intense and cover all the needed vibrational transitions. In fact, optical pumping is usually limited by the finite laser spectral linewidth Γ_L. The required irradiance density $I\Gamma_L$, where I is the laser irradiance, can be evaluated from a simple two-level (absorption and emission) model [61]. The model used in this study is based on calculating the resonant absorption rate γ for the RbCs molecular transition using a cutomized form of Einestein's absorption coefficient formula given by: $\gamma \sim \gamma_0 \left(\frac{\lambda}{500\ \text{nm}} \right)^3 \left(q_{v_X v_B} \times AF \right) \times I \left(\frac{\Gamma_L}{\Gamma} \right)$, where γ_0 is a constant that determines the magnitude of the absorption rate. The terms $q_{v_X v_B}$ and AF represent the Franck-Condon and angular factors, respectively [61]. The other variables are the laser wavelength λ, the normalized incident laser intensity I, and the natural linewidth of the transition Γ. Typically, for $\Gamma = \pi \times 2(10\ \text{MH})$, a 1 W laser with a linewidth of 10 nm (corresponding to roughly $\Gamma_L = \pi \times 2$ (10000 GH) at 500 nm) focused on 1 mm leads to an excitation rate of one photon absorbed every 3 μs. Thus, the full optical pumping probably takes hundreds of microseconds.

In the scheme we are describing, the light's coherence is not a concern; any sufficiently collimated source can be shaped and focused onto the molecular sample. We then have to choose a laser system that has a broadband spectrum.

3. Results and discussion

We assume that the molecules are formed in the ground electronic state via photoassociation [41, 42], which predominantly populates the lowest vibrational levels of the RbCs ground electronic state, $v_X < 20$. Starting from an initial uniform distribution of molecules over the vibrational levels $v_X = 1-10$, we simulated the vibrational optical pumping using a 1 W laser with a Gaussian spectral profile of 300 cm^{-1} (bandwidth), centered at 13660 cm^{-1}. The laser beam, with a waist of 0.3 mm, is assumed to uniformly cover the molecular sample. The corresponding laser spectrum is shown in Fig. 2a, where the frequencies associated with the transitions $v_X = 0 \rightarrow v_B$ have been removed to prevent excitation from the $v_X = 0$ level. It is not necessary to know the exact initial distribution of the molecular population, as repeated excitation and relaxation cycles effectively redistribute the population. This leads to a final distribution that is independent of the initial distribution, provided all the initially populated energy levels fall within the range of the pumping laser.

The result of this simulation is presented in Fig. 2b. As shown, a significant portion of the total molecular population – approximately 50% – is successfully pumped into the ground vibrational level after applying 2.5×10^4 laser pulses.

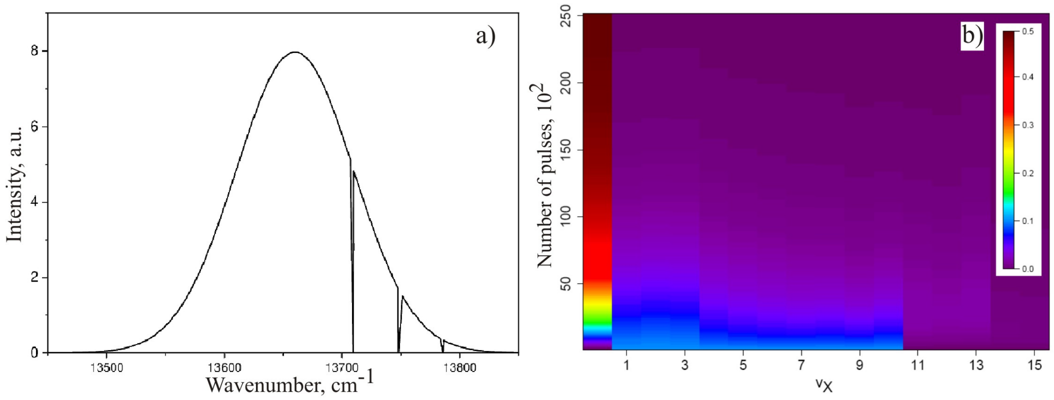

Fig. 2. Results of the simulation. (a) The laser spectrum used in the simulation. (b) The molecular population in each vibrational level v_X as a function of the number of pulses.

Fig. 3a illustrates the temporal evolution of the population at $v_X = 0$ level. The transfer of population to this level saturates after approximately 250 µs. Our results indicate that roughly 10 photons (corresponding to 5 absorption-emission cycles) are required to achieve vibrational cooling from the vibrational level $v_X \approx 10$.

The remaining 50% of the molecular population is transferred to higher vibrational levels unaffected by the laser, as the corresponding transitions fall outside the pumping laser pulse's spectral range. This result is further confirmed by simulating the vibrational cooling efficiency from several vibrational levels $v_X > 10$ to $v_X = 0$ using a five-times-larger laser bandwidth. Fig. 3b shows that the vibrational cooling efficiency increases to ~90%. In practice, we can use a supercontinuum laser that spans 0.4–2.3 µm with a uniform power

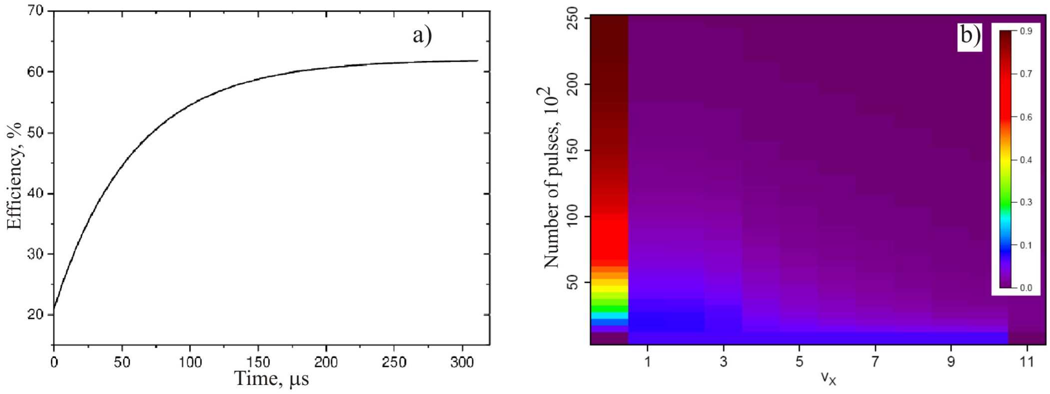

Fig. 3. (a) Time evolution of the population in $v_X = 0$ level. Saturation is reached after a typical time of 120µs. (b) Results of the simulation of the vibrational cooling. The population of the $v_X = 0$ level after 2.5 ×10^4 pulses is around 90%. The laser bandwidth is now five times larger than that of the previous pulses in Fig. 2.

density of approximately 50 mW/nm [62]. Alternatively, it may be more practical to use separate (diode) lasers to drive the required transitions. Broadband laser diodes or (tapered) amplifiers, with or without anti-reflective coatings, represent one of the simplest and most cost-effective solutions [38], offering relatively narrow bandwidths (on the order of tens of nanometers) combined with high spectral power density.

The idea of removing frequencies that correspond to (all) possible excitations of a particular vibrational level, to form a dark state, can be applied to any level v_X. Fig. 4 shows the case where the target vibrational levels are $v_X =$ 1 and 2, respectively. The simulation using a 300 cm^{-1} bandwidth laser predicts a total transfer of around 50% of molecules to $v_X = 1$ and $v_X = 2$ levels.

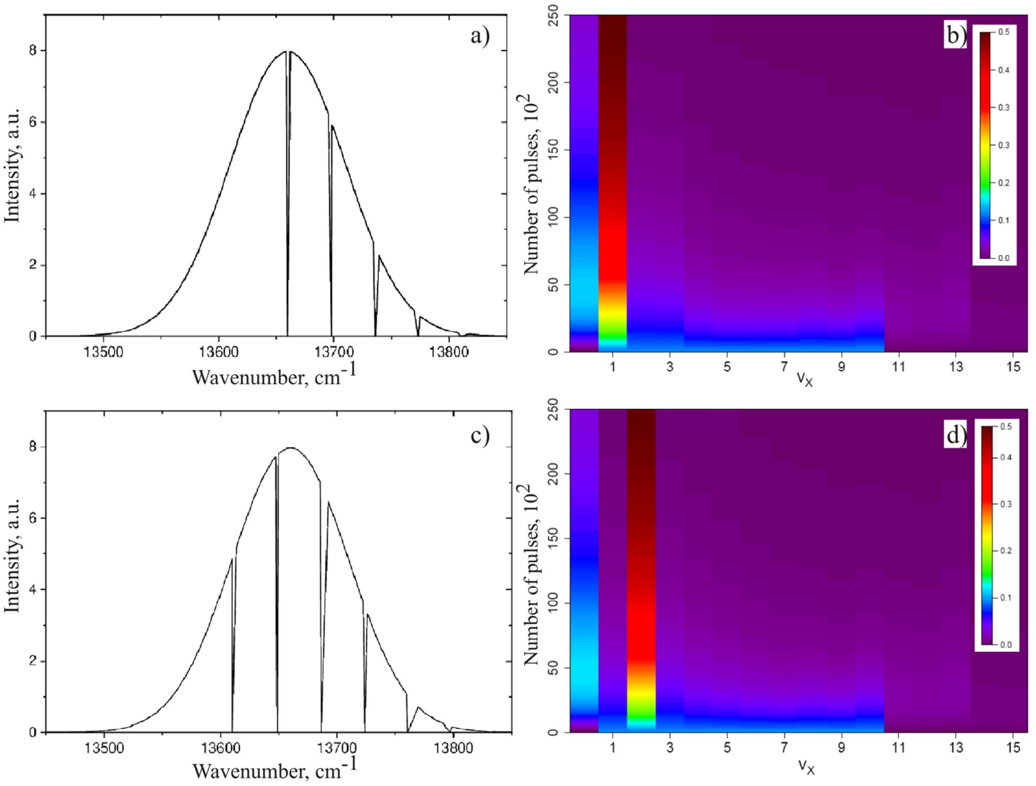

Fig. 4. The laser spectra (a,c) and corresponding molecular population in the $v_X = 1$ level (b) and the $v_X = 2$ level (d).

The vibrational dependence of an optical transition $v_B \leftarrow v_X$ between two electronic states is typically characterized by the corresponding FCF. Fig. 5 provides a useful reference for qualitatively predicting how the vibrational population may evolve. Starting from an initial vibrational level v_X, excitation to a level v_B is followed by spontaneous and efficient decay, predominantly near the inner Condon turning point, leading to the population of the ground vibrational level $v_{Xf} = 0$ (via point B). At the same time, excitation to this particular v_B level can also result in a significant population of higher vibrational levels due to decay occurring near the outer Condon turning point (via point C). A key factor in analyzing how molecules redistribute their internal energy is the position of point A in Fig. 5. This point corresponds to a specific vibrational level, $v_X(A)$, which, when excited to $v_B = 0$, exhibits minimal deexcitation to other vibrational levels. Consequently, an effective strategy for optical pumping involves pumping populations in $v_X(A)$, driving mainly transitions to $v_B = 0$. However, some FCFs, such as those between $v_X > 10$ and $v_B = 0$ in Fig. 5, are too small to ensure efficient excitation. As a result, to improve pumping efficiency, absorption transitions with $v_B \neq 0$ must also be considered and controlled.

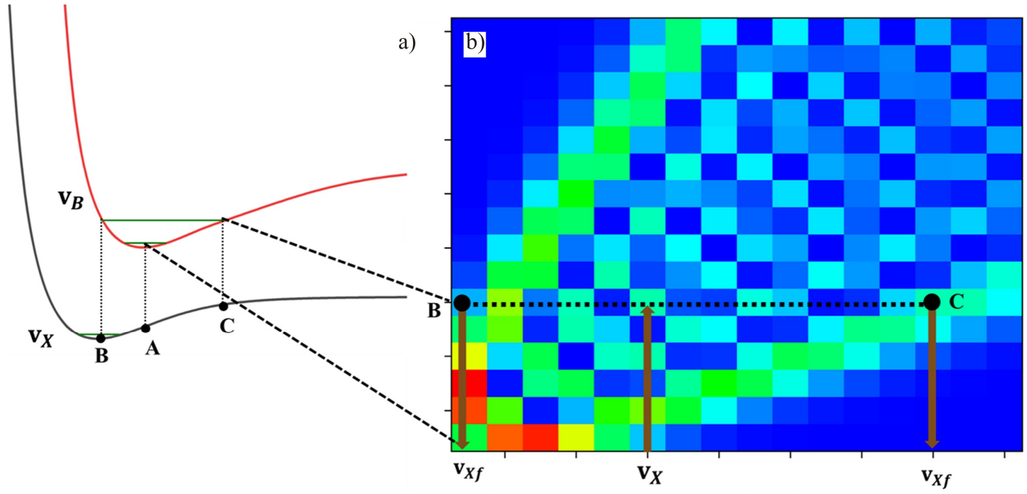

Fig. 5. (a) Schematics of the energy diagram of an electronic transition with (b) the corresponding FC matrix elements. The vibrational part is illustrated together with the FCFs for any vibrational $v_B \leftarrow v_X$ transition. When an initial level v_X is excited to a v_B state, spontaneous decay can occur via two pathways: (1) relaxation to $v_{Xf} = 0$ at the inner Condon point (path B), or (2) population transfer to higher vibrational levels at the outer Condon point (path C). The only exception occurs for the specific case of $v_X(A)$ excited to $v_B = 0$ (point A), where the population remains largely unchanged as spontaneous decay predominantly returns the system to its original level.

In this study, we explore the use of a tailored "comb" of laser frequencies, selected to drive transitions that efficiently pump from initially populated vibrational levels to a desired target state. One approach to selecting the set of excited states involves identifying those with the highest FCFs (with the target vibrational level). However, given the constraints of finite laser bandwidth, it becomes crucial to avoid populating high vibrational levels (as indicated by point C in Fig. 5) that fall outside the laser's effective range. Therefore, it is preferable to prioritize excitations involving vibrational levels on the "lower branch" of the FC parabola. With this strategy, when a molecule in a particular v_X level is excited, it can either decay to a lower vibrational level within the "lower branch" or return to the same v_X level via the "upper branch." In the latter case, the process can simply be repeated. This approach is illustrated in the simulation shown in Fig. 6, where the target vibrational levels are $v_X(A) = 0,1$. The initial population spans vibrational levels $v_X = 1$ to $v_X = 10$, and the laser bandwidth is set to 300 cm $^{-1}$. According to the simulation, after 2.5×10^4 laser pulses, approximately 70% and 60% of the population is transferred to $v_X = 0$ and $v_X = 1$, respectively. The corresponding laser spectra used for this simulation are also presented in Fig. 6.

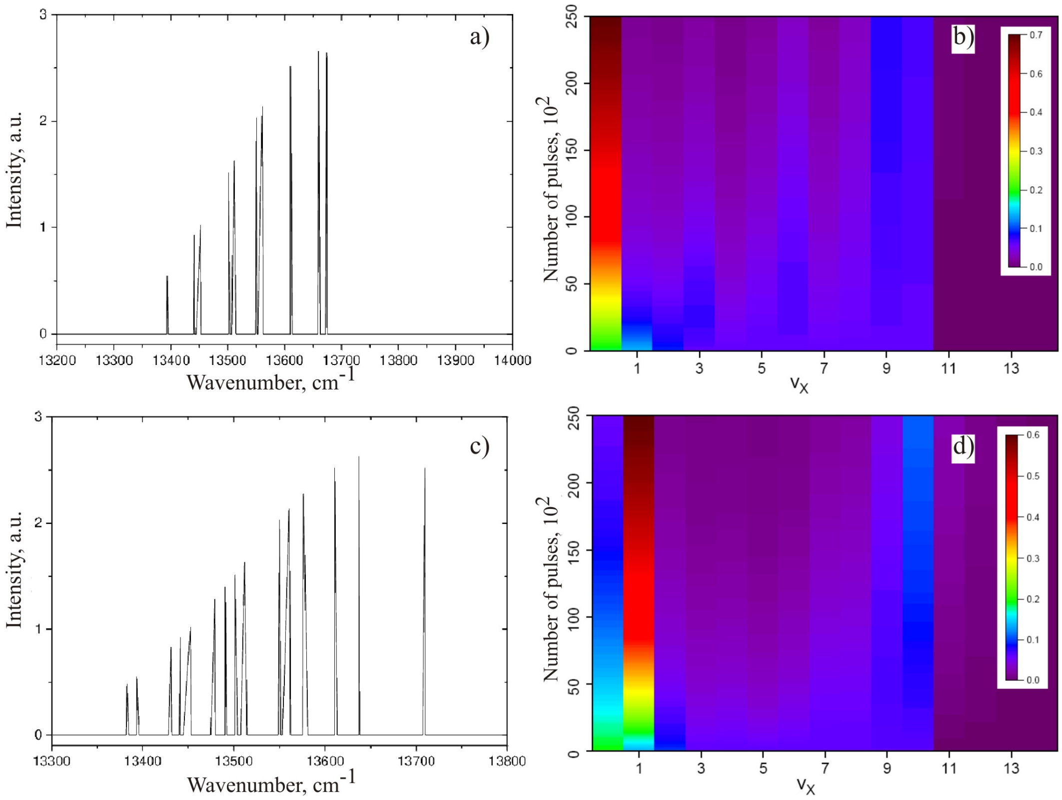

Fig. 6. Results of the simulation of the vibrational cooling. The shaped pulse used for the simulation for $v_X = 0$ (a) and $v_X = 1$ (b). The population at the $v_X = 0$ (b) and $v_X = 1$ (d) levels after 2.5×10^4 pulses is 70 % and 60 %, respectively.

4. Conclusion

The simulation results for the vibrational cooling of RbCs molecules via optical pumping show that up to 70% of the molecular population can be transferred to the ground vibrational level. This efficiency increases to nearly 90% with further optimization of laser shaping and the use of a broader laser spectrum. These improvements pave the way for using this optical pumping technique as a repumping mechanism in molecular laser cooling schemes. Additionally, trapping the cooled molecules in an optical potential opens new opportunities to explore collisional dynamics, which could provide insights into the feasibility of evaporative cooling or serve as a platform for studying controlled chemical reactions.

Funding. The authors received no financial support for this research.

Conflict of interest. Authors declare no conflict of interest.

Data availability. The datasets used and/or analysed during the current study are available from the corresponding author on reasonable request.

Author contribution. R.H. designed the model and the computational framework and analyzed the data. O.A carried out the simulations. R.H and O.A wrote the manuscript.

References

1. Carr, L. D., DeMille, D., Krems, R. V., & Ye, J. (2009). Cold and ultracold molecules: science, technology and applications. *New Journal of Physics*, *11*(5), 055049.

2. Jin, D. S., & Ye, J. (2012). Introduction to ultracold molecules: new frontiers in quantum and chemical physics. *Chemical Reviews*, *112*(9), 4801-4802.
3. Quéméner, G., & Julienne, P. S. (2012). Ultracold molecules under control!. *Chemical Reviews*, *112*(9), 4949-5011.
4. Landisman, C. E., & Connors, B. W. (2005). Long-term modulation of electrical synapses in the mammalian thalamus. *Science*, *310*(5755), 1809-1813.
5. Tannor, D. (1999). Laser cooling of internal degrees of freedom of molecules by dynamically trapped states. *Faraday Discussions*, *113*, 365-383.
6. Morigi, G., Pinkse, P. W., Kowalewski, M., & de Vivie-Riedle, R. (2007). Cavity cooling of internal molecular motion. *Physical Review Letters*, *99*(7), 073001.
7. Bartana, A., Kosloff, R., & Tannor, D. J. (1993). Laser cooling of molecular internal degrees of freedom by a series of shaped pulses. *The Journal of Chemical Physics*, *99*(1), 196-210.
8. Baranov, M., Góral, K., Santos, L., & Lewenstein, M. (2002). Ultracold dipolar gases–a challenge for experiments and theory. *Physica Scripta*, *2002* (T102), 74.
9. Góral, K., Santos, L., & Lewenstein, M. (2002). Quantum phases of dipolar bosons in optical lattices. *Physical Review Letters*, *88*(17), 170406.
10. Barnett, R., Petrov, D., Lukin, M., & Demler, E. (2006). Quantum magnetism with multicomponent dipolar molecules in an optical lattice. *Physical Review Letters*, *96*(19), 190401.
11. Micheli, A., Pupillo, G., Büchler, H. P., & Zoller, P. (2007). Cold polar molecules in two-dimensional traps: Tailoring interactions with external fields for novel quantum phases. *Physical Review A – Atomic, Molecular, and Optical Physics*, *76*(4), 043604.
12. Gregory, P. D., Aldegunde, J., Hutson, J. M., & Cornish, S. L. (2016). Controlling the rotational and hyperfine state of ultracold $Rb^{87}Cs^{133}$ molecules. *Physical Review A*, *94*(4), 041403.
13. Molony, P. K., Gregory, P. D., Ji, Z., Lu, B., Köppinger, M. P., Le Sueur, C. R., Blackley, C. L., Hutson, J. M., & Cornish, S. L. (2014). Creation of ultracold $Rb^{87}Cs^{133}$ molecules in the rovibrational ground state. *Physical Review Letters, 113*(25), 255301.
14. Park, J. W., Will, S. A., & Zwierlein, M. W. (2015). Ultracold dipolar gas of fermionic Na 23 K 40 molecules in their absolute ground state. *Physical Review Letters*, *114*(20), 205302.
15. Guo, M., Zhu, B., Lu, B., Ye, X., Wang, F., Vexiau, R., Bouloufa-Maafa, N., Quéméner, G., Dulieu, O., & Wang, D. (2016). Creation of an ultracold gas of ground-state dipolar $Na^{23}Rb^{87}$ molecules. *Physical Review Letters, 116*(20), 205303.
16. Ospelkaus, S., Ni, K. K., Wang, D., de Miranda, M. H. G., Neyenhuis, B., Quéméner, G., Julienne, P. S., Bohn, J. L., Jin, D. S., & Ye, J. (2010). Quantum-state controlled chemical reactions of ultracold potassium-rubidium molecules. *Science, 327*(5967), 853-857.
17. Thorsheim, H. R., Weiner, J., & Julienne, P. S. (1987). Laser-induced photoassociation of ultracold sodium atoms. *Physical Review Letters*, *58*(23), 2420.
18. Maioli, P., Meunier, T., Gleyzes, S., Auffèves, A., Nogues, G., Brune, M., Raimond, J. M., & Haroche, S. (2005). Nondestructive Rydberg atom counting with mesoscopic fields in a cavity. *Physical Review Letters, 94*(11), 113601.
19. Jones, K. M., Tiesinga, E., Lett, P. D., & Julienne, P. S. (2006). Ultracold photoassociation spectroscopy: Long-range molecules and atomic scattering. *Reviews of Modern Physics*, *78*(2), 483-535.
20. Aikawa, K., Akamatsu, D., Hayashi, M., Oasa, K., Kobayashi, J., Naidon, P., Ueda, M., & Inouye, S. (2010). Coherent transfer of photoassociated molecules into the rovibrational ground state. *Physical Review Letters, 105*(20), 203001.
21. Patterson, D., & Doyle, J. M. (2007). Bright, guided molecular beam with hydrodynamic enhancement. *The Journal of Chemical Physics*, *126*(15).
22. Yamakita, Y., Takahashi, R., Ohno, K., Procter, S. R., Maguire, G., & Softley, T. P. (2007). Cooling effects in the Stark deceleration of Rydberg atoms/molecules with time-dependent electric fields. In *Journal of Physics: Conference Series* (Vol. 80, No. 1, p. 012045). IOP Publishing.
23. Bethlem, H. L., Berden, G., & Meijer, G. (1999). Decelerating neutral dipolar molecules. *Physical Review Letters*, *83*(8), 1558.
24. van Veldhoven, J., Bethlem, H. L., & Meijer, G. (2005). AC electric trap for ground-state molecules. *Physical Review Letters*, *94*(8), 083001.
25. Narevicius, E., Libson, A., Parthey, C. G., Chavez, I., Narevicius, J., Even, F. U., & Raizen, M. G. (2008). Stopping supersonic beams with a series of pulsed electromagnetic coils: an atomic coilgun. *Physical Review Letters*, *100*(9), 093003.
26. Sawyer, B. C., Lev, B. L., Hudson, E. R., Stuhl, B. K., Lara, M., Bohn, J. L., & Ye, J. (2007). Magnetoelectrostatic trapping of ground state OH molecules. *Physical Review Letters*, *98*(25), 253002.
27. Vanhaecke, N., Meier, U., Andrist, M., Meier, B. H., & Merkt, F. (2007). Multistage Zeeman deceleration of hydrogen atoms. *Physical Review A – Atomic, Molecular, and Optical Physics*, *75*(3), 031402.
28. Fulton, R., Bishop, A. I., Shneider, M. N., & Barker, P. F. (2006). Controlling the motion of cold molecules with deep periodic optical potentials. *Nature Physics*, *2*(7), 465-468.
29. DeMille, D. (2002). Quantum computation with trapped polar molecules. *Physical Review Letters, 88*(6), 067901.

30. DeMille, D., Doyle, J. M., & Sushkov, A. O. (2017). Probing the frontiers of particle physics with tabletop-scale experiments. *Science, 357*(6355), 990–994.
31. Gorshkov, A. V., Manmana, S. R., Chen, G., Demler, E., Lukin, M. D., & Rey, A. M. (2011). Quantum magnetism with polar alkali-metal dimers. *Physical Review A, 84*(3), 033619.
32. Hudson, E. R., Lewandowski, H. J., Sawyer, B. C., & Ye, J. (2006). Cold molecule spectroscopy for constraining the evolution of the fine structure constant. *Physical Review Letters, 96*(14), 143004.
33. Hughes, M., Frye, M. D., Sawant, R., Bhole, G., Jones, J. A., Cornish, S. L., Tarbutt, M. R., Hutson, J. M., Jaksch, D., & Mur-Petit, J. (2020). Robust entangling gate for polar molecules using magnetic and microwave fields. *Physical Review A, 101*(6), 062308.
34. Macià, A., Hufnagl, D., Mazzanti, F., Boronat, J., & Zillich, R. E. (2012). Excitations and stripe phase formation in a two-dimensional dipolar Bose gas with tilted polarization. *Physical Review Letters, 109*(23), 235307.
35. McDonald, M., McGuyer, B. H., Apfelbeck, F., Lee, C.-H., Majewska, I., Moszynski, R., & Zelevinsky, T. (2016). Photodissociation of ultracold diatomic strontium molecules with quantum state control. *Nature, 535*(7611), 122–126.
36. Yelin, S. F., Kirby, K., & Côté, R. (2006). Schemes for robust quantum computation with polar molecules. *Physical Review A, 74*(5), 050301.
37. Sage, J. M., Sainis, S., Bergeman, T., & DeMille, D. (2005). Optical production of ultracold polar molecules. *Physical Review Letters*, *94*(20), 203001.
38. Ni, K. K., Ospelkaus, S., De Miranda, M. H. G., Pe'er, A., Neyenhuis, B., Zirbel, J. J., Kotochigova, S., Julienne, P. S., Bohn, J. L., Jin, D. S., & Ye, J. (2008). A high phase-space-density gas of polar molecules. *Science, 322*(5899), 231-235.
39. Banerjee, J., Rahmlow, D., Carollo, R., Bellos, M., Eyler, E. E., Gould, P. L., & Stwalley, W. C. (2012). Direct photoassociative formation of ultracold KRb molecules in the lowest vibrational levels of the electronic ground state. *Physical Review A – Atomic, Molecular, and Optical Physics*, *86*(5), 053428.
40. Deiglmayr, J., Grochola, A., Repp, M., Mörtlbauer, K., Glück, C., Lange, J., Dulieu, O., Wester, R., & Weidemüller, M. (2008). Formation of ultracold polar molecules in the rovibrational ground state. *Physical Review Letters, 101*(13), 133004.
41. Bruzewicz, C. D., Gustavsson, M., Shimasaki, T., & DeMille, D. (2014). Continuous formation of vibronic ground state RbCs molecules via photoassociation. *New Journal of Physics*, *16*(2), 023018.
42. Fioretti, A., & Gabbanini, C. (2013). Experimental study of the formation of ultracold RbCs molecules by short-range photoassociation. *Physical Review A – Atomic, Molecular, and Optical Physics*, *87*(5), 054701.
43. Kerman, A. J., Sage, J. M., Sainis, S., Bergeman, T., & DeMille, D. (2004). Production of Ultracold, Polar RbCs* Molecules via Photoassociation. *Physical review letters*, *92*(3), 033004.
44. Liu, Y., Gong, T., Ji, Z., Wang, G., Zhao, Y., Xiao, L., & Jia, S. (2019). Production of ultracold ^{85}Rb^{133}Cs molecules in the lowest ground state via the B$^1\Pi^1$ short-range state. *The Journal of Chemical Physics*, *151*(8).
45. Zabawa, P., Wakim, A., Haruza, M., & Bigelow, N. P. (2011). Formation of ultracold X 1 Σ+(v′′= 0) NaCs molecules via coupled photoassociation channels. *Physical Review A – Atomic, Molecular, and Optical Physics*, *84*(6), 061401.
46. Stwalley, W. C., Banerjee, J., Bellos, M., Carollo, R., Recore, M., & Mastroianni, M. (2009). Resonant coupling in the heteronuclear alkali dimers for direct photoassociative formation of X(0,0) ultracold molecules. *The Journal of Physical Chemistry A, 114*(1), 81–86.
47. Cournol, A., Pillet, P., Lignier, H., & Comparat, D. (2018). Rovibrational optical pumping of a molecular beam. *Physical Review A*, *97*(3), 031401.
48. Courageux, T., Cournol, A., Comparat, D., de Lesegno, B. V., & Lignier, H. (2022). Efficient rotational cooling of a cold beam of barium monofluoride. *New Journal of Physics*, *24*(2), 025007.
49. Sofikitis, D., Fioretti, A., Weber, S., Viteau, M., Chotia, A., Horchani, R., Akan, D., & Pillet, P. (2009). Broadband vibrational cooling of cold cesium molecules: theory and experiments. *Chinese Journal of Chemical Physics, 22*(2), 149.
50. Sofikitis, D., Weber, S., Fioretti, A., Horchani, R., Allegrini, M., Chatel, B., & Pillet, P. (2009). Molecular vibrational cooling by optical pumping with shaped femtosecond pulses. *New Journal of Physics, 11*(5), 055037.
51. Fioretti, A., Sofikitis, D., Horchani, R., Li, X., Pichler, M., Weber, S., Horchani, R., & Pillet, P. (2009). Cold cesium molecules: from formation to cooling. *Journal of Modern Optics, 56*(18-19), 2089-2099.
52. Sofikitis, D., Horchani, R., Li, X., Pichler, M., Allegrini, M., Fioretti, A., & Pillet, P. (2009). Vibrational cooling of cesium molecules using noncoherent broadband light. *Physical Review A, 80*(5), 051401.
53. Sofikitis, D., Fioretti, A., Weber, S., Horchani, R., Pichler, M., Li, X., & Pillet, P. (2010). Vibrational cooling of cold molecules with optimised shaped pulses. *Molecular Physics, 108*(6), 795-810.
54. Lignier, H., Fioretti, A., Horchani, R., Drag, C., Bouloufa, N., Allegrini, M., Chotia, A., & Comparat, D. (2011). Deeply bound cold caesium molecules formed after resonant coupling. *Physical Chemistry Chemical Physics, 13*(42), 18910-18920.
55. Manai, I., Horchani, R., Lignier, H., Pillet, P., Comparat, D., Fioretti, A., & Allegrini, M. (2012). Rovibrational cooling of molecules by optical pumping. *Physical review letters*, *109*(18), 183001.

56. Manai, I., Horchani, R., Hamamda, M., Fioretti, A., Allegrini, M., Lignier, H., Bouloufa, N., & Comparat, D. (2013). Laser cooling of rotation and vibration by optical pumping. *Molecular Physics, 111*(12-13), 1844-1854.
57. Horchani, R. (2016). Cold molecules: Formation, ro-vibrational cooling and electronic conversion. *International Journal of Modern Physics B*, *30*(14), 1630010.
58. Viteau, M., Chotia, A., Allegrini, M., Bouloufa, N., Dulieu, O., Comparat, D., & Pillet, P. (2008). Optical pumping and vibrational cooling of molecules. *Science*, *321*(5886), 232-234.
59. Wakim, A., Zabawa, P., Haruza, M., & Bigelow, N. P. (2012). Luminorefrigeration: vibrational cooling of NaCs. *Optics Express*, *20*(14), 16083-16091.
60. Brif, C., Chakrabarti, R., & Rabitz, H. (2010). Control of quantum phenomena: past, present and future. *New Journal of Physics*, *12*(7), 075008.
61. Comparat, D. (2014). Molecular cooling via Sisyphus processes. *Physical Review A*, *89*(4), 043410.
62. Travers, J. C. (2010). Blue extension of optical fibre supercontinuum generation. *Journal of Optics*, *12*(11), 113001.

Al Kharusi, O., Horchani, R., Okorie, U. S., Ikot, A. N. (2026). Vibrational Cooling of RbCs molecules**.** *Ukrainian Journal of Physical Optics*, *27*(2), 02023–02034l.
doi: 10.3116/16091833/Ukr.J.Phys.Opt.2026.02023

Анотація. *Теоретично досліджене коливне охолодження молекул RbCs, утворених внаслідок фотоасоціації атомів Rb та Cs. Холодні молекули, спочатку розподілені по кількох коливних рівнях, можуть бути переведеними на певний коливний рівень синглетного основного електронного стану* $X^1\sum^+$*. Це досягається шляхом багаторазового оптичного нагнітання лазерним випромінюванням зі спектром, достатньо широким для збудження всіх заселених коливних рівнів крім цільового. Як свідчать отримані результати, ефективність цього методу охолодження може наближатися до 100%.*

Ключові слова: *оптичне нагнітання, коливне охолодження, молекули*